Asian Journal of Chemistry; Vol. 32, No. 3 (2020), 501-507

ASIAN JOURNAL OF CHEMISTRY

https://doi.org/10.14233/ajchem.2020.22357

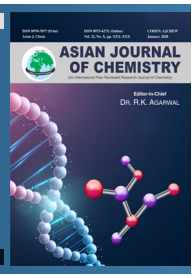

Study of Green and Chemical Methods for Synthesis of Nano Spinel $MgFe_2O_4$ and its Study on Degradation of Rose Bengal Dye

KRUSHITHA SHETTY[1], B.S. PRATHIBHA[2,*], DINESH RANGAPPA[1,*], K.S. ANANTHARAJU[3], H.P. NAGASWARUPA[4] and VINAY GANGARAJU[1]

[1]Department of Nanotechnology, VIAT, Visvesvaraya Technological University, PG Center, Muddenahalli, Chikkaballapur-562103, India
[2]Department of Chemistry, B.N.M. Institute of Technology, Bangalore-560070, India
[3]Department of Chemistry, Dayanand Sagar College of Engineering, Shavige Malleshwara Hills, Kumaraswamy Layout, Bangalore-560078, India
[4]P.G. Department of Chemistry, Davanagere University, Davanagere-577001, India

*Corresponding authors: E-mail: pratbnmit@gmail.com; dineshrangappa@gmail.com

Received: 25 July 2019; *Accepted*: 29 September 2019; *Published online*: 31 January 2020; AJC-19749

$MgFe_2O_4$ nanoferrites were synthesized by sol-gel and solution combustion synthesis (SCS) methods through green and chemical methods. Green and chemical methods for sol-gel were processed with use of lemon extract and citric acid, respectively. A green and chemical method for solution combustion synthesis was followed by using *Phyllanthus acidus* leaf extract and urea, respectively. The influence of synthesis approach on the behaviour of prepared nanoferrites were studied using powder X-ray diffraction (PXRD), Fourier transform infrared spectroscopy (FT-IR), scanning electron microscopy (SEM) and UV visible spectroscopy, vast variation in particle size, crystallinity, electrochemical and photocatalytic activity of the nanoferrites synthesized by various methods were witnessed. Powder X-ray diffraction (PXRD) result of prepared nanoferrites acquired by green and chemical approaches clarified phase structure as spinel and the crystalline size found to be around 11-24 nm. The spinel surface morphology was witnessed for the synthesized nanoferrites. The tetrahedral and octahedral sites of the prepared nanoferrites were confirmed by FTIR spectra. $MgFe_2O_4$ nanoferrites synthesized by green sol-gel approach exposed superior electrochemical activity by possessing very less charge transfer resistance. The results of EIS were correlated with the photocatalytic degradation of Rose Bengal dye. Photocatalytic property of the prepared nanoferrites was examined for photodegradation of Rose Bengal dye under UV-light.

Keywords: Nanoferrites, Sol-gel, Solution combustion synthesis, Photocatalytic property, *Phyllanthus acidus*, Rose Bengal dye.

INTRODUCTION

Nanoferrites are one of the beneficial ceramic semiconductor materials ever revealed. Since, it is less cost and ease of synthesis process, it can be used as substitute for any ceramic materials for different application such as cancer treatment, isolators, circulators, microwave absorbing materials, magnetic resonance imaging, TV yolks, noise filters, memory devices, transformer communications [1-4]. Nanoferrite $MgFe_2O_4$ is a vigorous nanomaterial which has vast applications in different fields of heterogeneous catalysis, adsorption, magnetic technologies and sensors [5].

In recent times, the demand for photocatalyst for the degradation of several types of dyes has been increased. To enhance the optic, electrochemical and photocatalytic properties of prepared materials, researchers have concentrated on various studies. In order to achieve these properties various techniques are made use to synthesize nanoferrites.

Various chemical approaches have been used to synthesize nanoferrites like hydrothermal methods [6], micelle routes combustion [7], sol-gel [8] and co-precipitation [9] had been used to prepare nanoferrites in the presence of ambient conditions. Nanoferrites prepared by such methods hold moderate purity and chemical homogeneity.

In general, nanoferrites synthesized using sol-gel route displays more crystallite size and high purity and are achieved in a comparatively less processing duration. Furthermore, it retains the benefit of better stoichiometric control with large yield [10]. Solution combustion synthesis (SCS) is a fast, appropriate and easy technique for synthesizing the nanoferrites of

size ranging from 1-100 nm. Starting materials of this method demands mixture of fuels (glycine urea, hydrazides) and oxidizers (nitrates). This technique depends on the volume or layer by layer self-propagating combustion modes.

Chemical methods for the preparation of nanoferrites are much costly, energy intensive and because of the use of toxic reagents impose environmental risks. To evade these demerits, a novel upcoming extension of nanotechnology *i.e*. green nanotechnology is the center of research attraction. It offers an eco-friendly and cost effective for production of novel nanomaterials using plant extracts. In recent times, biomaterials have been used for the preparation of nanoparticles predominantly nanoferrites. Tragacanth gum [11], aloe vera extract [12] have been used in the synthesis of ferrite nanoparticles. Also, *Citrus limon* extract has been used as de-agglomerating and reducing agent for the synthesis of silver nanoparticles [13]. Citrus extracts contains high amount of ascorbic acid and citric acid acts as exceptional reducing agents [14,15]. Also added motive behind selecting this particular plant is its less cost and readily available fruit. Solution combustion synthesis (SCS) methods have been accomplished by using biomaterials such as extracts of ginger root and cardamom seeds [16]. *Phyllanthus acidus* is a small, glabrous tree native to the coastal region of north-east Brazil. The leaf extract is used to cure skin, asthma, hypertension, coughs, emetic, cathartic diseases and as a food [17]. Nevertheless, a use of *Phyllanthus acidus* is not stated in the literature for the preparation of ferrite nanoparticles.

$MgFe_2O_4$ nanoferrite has efficient band gap of ~ 2.0 eV, that helps to capture ultraviolet light and also fewer photosensitive to the anodic corrosion [18-20]. These nanoferrite has revealed various uses as magnetic recording media, photocatalyst, adsorption and heterogeneous sensors [21]. It is revealed that oxygen vacancy defects present on the external layer of $MgFe_2O_4$ nanoferrites leads to trap the photo-excited electrons from the nanoferrite and increases the charge recombination duration of photo-excited electron-hole pairs, which permit the positive charge to produce hydroxyl and superoxide radicals, thereby improving the photocatalytic performance.

In this work, we present the role of green and chemical preparation methods on the crystalline structure, electrochemical activity and photocatalytic performance. Present objective is to synthesize nanoferrites of $MgFe_2O_4$ *via* sol-gel and solution combustion synthesis routes *via* green and chemical routs and to relate their comparative features. Furthermore, discover the nanoferrites that possess improved electrochemical and photocatalytic performance. Prepared nanoferrites were further examined by UV-vis spectroscopy, FTIR, SEM and PXRD. Additionally, the electrochemical and photocatalytic activity was examined in the presence of UV light by degradation of Rose Bengal dye. To our best of knowledge, no work has been reported on synthesis of $MgFe_2O_4$ by green and chemical synthesis using *Phyllanthus acidus* leaf and lemon extract.

EXPERIMENTAL

The chemicals used for preparation of nanoferrites such as magnesium nitrate, ferric nitrate, Rose Bengal dye and urea were procured from Sigma-Aldrich, U.S.A. The entire precursor materials were of analytical grade and used as received without additional purification.

Preparation of citrus lemon extract: Citrus lemon fruit was washed cleanly with distilled water and then squeezed to extract the juice of it. Further, 5 mL of citrus lemon extract was diluted with 50 mL of double distilled water.

Green sol-gel route: For the preparation $MgFe_2O_4$ nanoferrite, 0.5 M of ferric nitrate, 0.25 M of magnesium nitrate and 0.25 M of citric acid were taken with 200 mL of deionized water. This reaction mixture was stirred for 2 h at 60 ºC to attain uniform mixture and sol pH was retained at 6. The darkish brown tinted sol was formed. The stable reaction mixture was subjected to sudden increase in temperature to 80 ºC. The dark brown coloured sol was transformed into transparent thick black gel. Further, thick gel was placed in muffle furnace at 200 ºC for 2 h and final product obtained was fluffy, brown coloured $MgFe_2O_4$ nanoferrite. To prepare $MgFe_2O_4$ *via* green sol-gel method, citric acid was replaced by citrus lemon extract for the above procedure.

Preparation of *Phyllanthus acidus* leaf extract: *P. acidus* leaves were obtained locally and the fresh leaves were cleaned with deionized water in order to eliminate any possible contaminations and dust particles and then finally washed with ethanol. The leaves extract were powdered by a sterile electric blender to acquire a fine powder and collected in sterile polyethylene bags prior to its use.

Green combustion method: Ferric nitrate, magnesium nitrate as oxidizer and urea as fuel were taken in stoichiometric quantity. For stoichiometric redox mechanism among a fuel and an oxidizer, *i.e*. the relation between the net reduction valencies of nitrates to the net oxidization valencies of fuel ratio has to be one. The metal nitrates and fuel were taken in minimum amount of deionized water and continuously mixed to attain homogeneous solution. Further, reaction mixture was placed in preheated muffle furnace at 550 ºC. After a while, a solution mixture was transformed into brown colour viscous solution. Furthermore, the huge quantity of fumes evolved and a fluffy mass was formed. Green combustion was processed by using *Phyllanthus acidus* leaf extract as a substitute for urea.

RESULTS AND DISCUSSION

The characterization of prepared nanoferrites was followed by different techniques. PXRD technique was accompleshed with Rigaku Ultima IV(Japan) ray diffraction diffractometer using Cu *K*α radiation (λ = 0.15407 nm) over a range of 10º to 70º at 40 kV and 30 mA. The scanning electron microscopy (SEM) (Hitachi SU1510) was utilized to obtain the external morphology of the prepared samples. The FTIR analysis was performed using Perkin-Elmer spectrometer (spectrum 1000) to examine the functional groups present in the prepared samples. UV-DRS analysis and absorption spectra was acquired by UV-Vis spectrophotometer (Perkin-Elmer spectrophotometer λ 250) furnished with integrating sphere application.

PXRD analysis: The reflections identified in PXRD spectra of $MgFe_2O_4$ sol-gel, green sol-gel and combustion, green combustion routes comprised of planes [440], [511], [422], [400], [311] and [220] (Fig. 1). All the identified planes established by specimens are totally allocated to the simple cubic phase structure of $MgFe_2O_4$ with JCPDS card No. 88-1935. The intensity of [422] plane observed to be more intense in nanoferrite synthesized by sol-gel than solution combustion synthesis

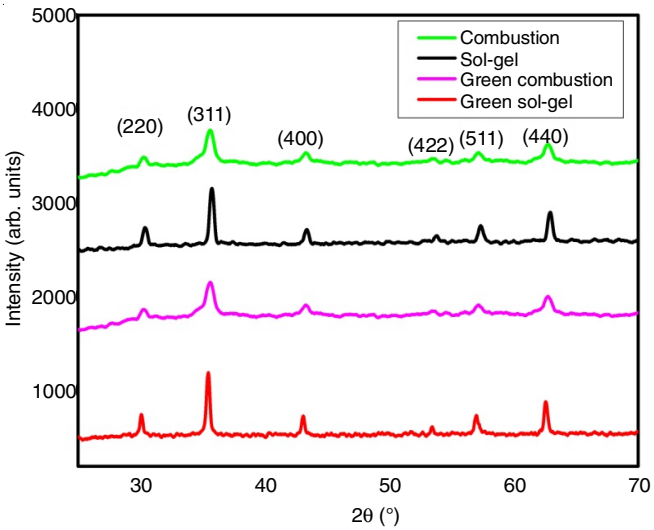

Fig. 1. XRD pattern for $MgFe_2O_4$ nanoferrites synthesized by sol-gel, green sol-gel and SCS, green SCS routes

(SCS). It is clearly observed that the peaks were narrower in green sol-gel PXRD spectra. This result may be observed due to three features such as lattice domain size distribution, micro strains (deformation of the lattice) and faulting (extended defects). If the specimens comprises no defects and strains then the broad peaks are result of lattice size distribution [22]. The particle size of prepared nanoferrites was estimated using Scherrer′s formula $D = k\lambda/\beta\cos\theta$ [23]; where θ is the diffraction angle, β is the full width at half maximum of the plane, λ is the wavelength of X- ray (0.15418 nm) and k is constant (shape factor, around 0.90). If the size of the particle is less then the surface area of nanoparticles are expected to be high. The structural parameters *viz.* stacking fault (SF) and dislocation density (δ) are also tabulated in Table-1. Therefore, the result confirms that synthesized green sol-gel $MgFe_2O_4$ nanoferrite has less size that may lead to larger surface area which enhances the contact area of dye with the photocatalyst. Thereby increases the photocatalytic performance of the green sol-gel $MgFe_2O_4$ nanoferrite.

TABLE-1
STRUCTURAL PARAMETERS FOR $MgFe_2O_4$ NANOFERRITES SYNTHESIZED BYSOL-GEL, GREEN SOL-GEL AND SCS, GREEN COMBUSTION ROUTES

Specimens	FWHM	Average particle size (nm)	δ (10^{15} lin m^{-2})	SF × 10^{-3}
SCS	0.4202	22.5	1.7934	0.3626
Sol-gel	0.7144	13.4	6.1000	0.4472
Green SCS	0.4030	20.0	1.6544	0.4181
Green sol-gel	0.7291	10.0	7.4270	0.3887

SEM analysis: The SEM analysis was accomplished to study the external morphology of prepared $MgFe_2O_4$ (Fig. 2a-d) at various magnifications. It was observed that the prepared nanoferrites showed flake type morphology which was non-uniform in shape. Sol-gel and green sol-gel prepared nanoferrites

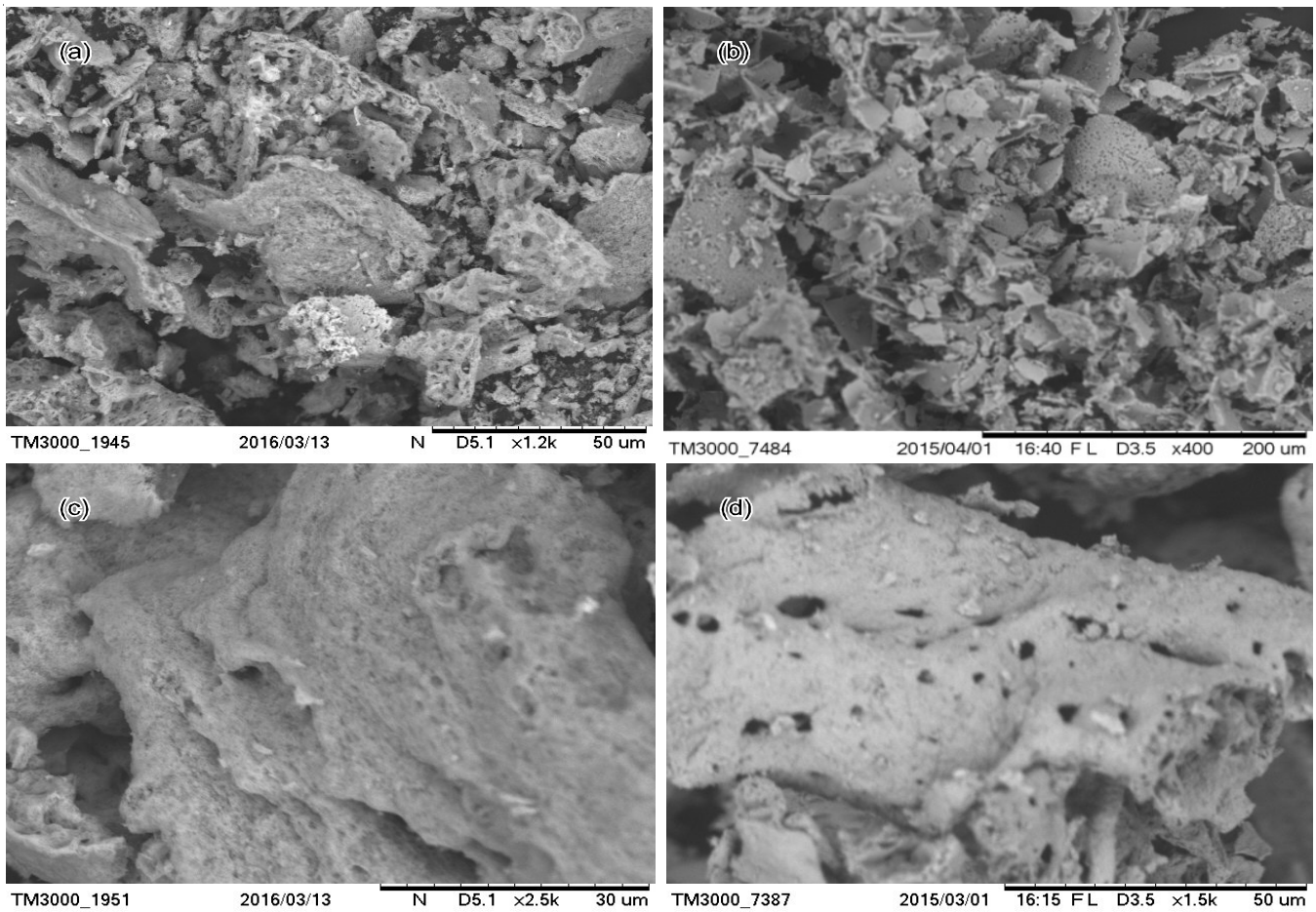

Fig. 2. SEM images for $MgFe_2O_4$ nanoferrites prepared by (a) sol-gel, (b) green sol-gel and (c) SCS, (d) green SCS methods

presented very less clusters with porous morphology (Fig. 2a-b). As seen in Fig. 2c-d, the grain size and morphology of nanoferrites appear to be uneven and contains few clusters, which are expected for both SCS and green SCS route. From the primary interpretations of microscopy photographs, it is concluded that the crystelline size of nanoferrites synthesized *via* SCS route is considerably affected.

FTIR analysis: As shown in Fig. 3, the prepared samples were subjected to FTIR analysis in the range 4000-400 cm^{-1}. With the use of IR illumination, the bands in the functional groups were identified by the study of its molecular/atomic vibrations is a remarkable proof [24]. Peaks around 630-450 cm^{-1} resulted due to the metal ionic vibrations. The two high intense absorption peaks were witnessed which are accredited to the frequencies of tetrahedral and octahedral sites at ~418 and ~549 cm^{-1} [25]. Peak identified at ~1470 cm^{-1} was ascribed to the bending frequency of C-H group. The band at ~3327 cm^{-1} was identified to the (O-H) hydroxyl group [26,27]. The band around 1710 cm^{-1} was due to the hydroxyl group bending vibrations of water molecules present on surface of nanoferrites.

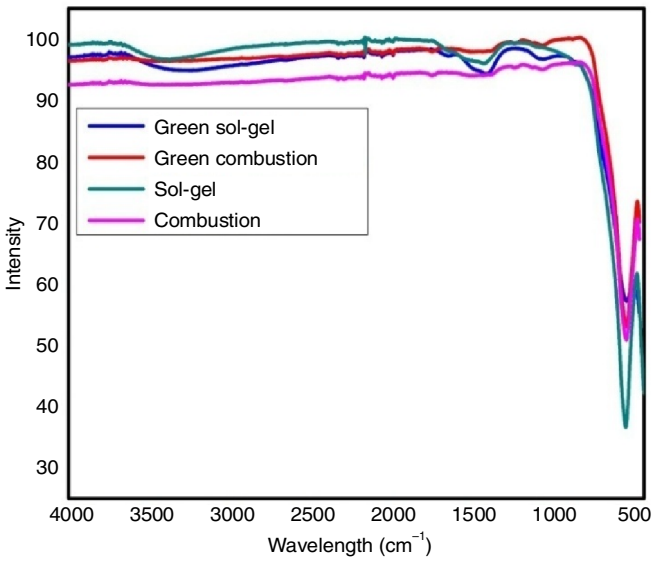

Fig. 3. FTIR for $MgFe_2O_4$ nanoferrites prepared by sol-gel, green sol-gel, SCS and green SCS methods

DRS analysis: Diffuse reflectance spectroscopy (DRS) was used to examine the absorbance and band gap. The UV-DRS data was obtained in the wavelength range around 200-800 nm. The wavelength and its absorbance acquired from the DRS analysis for the sample (Fig. 4). At a corresponding wavelength of 499 nm maximum absorbance was observed, which falls in visible light region of solar spectrum. From the acquired results, it is evidently observed that green sol-gel nanoferrites create blue shift near the reflectance edge of $MgFe_2O_4$ and causes decline in the band gap energy.

Kulbeka Munk function is used to obtain absorption spectra for the prepared $MgFe_2O_4$ nanoferrites to determine the E_g and is known by

$$F(R) = \frac{1-R2}{2R} \quad (1)$$

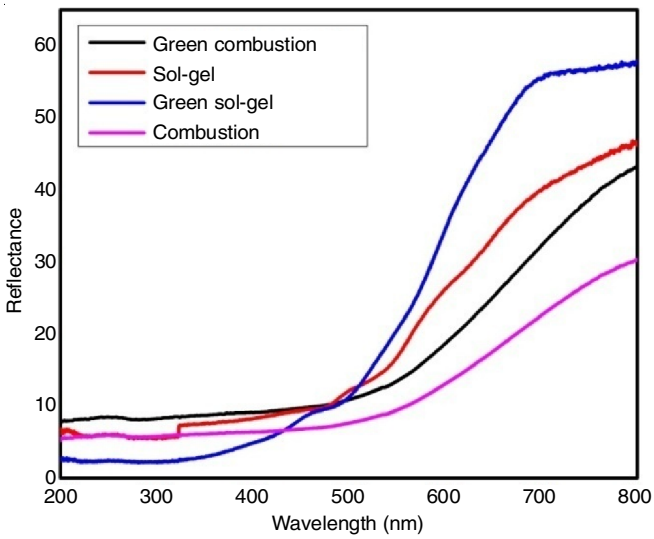

Fig. 4. Reflectance spectra for $MgFe_2O_4$ nanoferrites prepared by sol-gel, green sol-gel, SCS and green SCS methods

Then Tauc relation is restructured from the Kulbeka Munk relation to obtain eqn. 2

$$[F(R)h\nu]2 = C(h\nu - Eg) \quad (2)$$

Here E_g = energy band gap C; hν = photon energy, a proportionality constant as displayed in Fig. 4, $(F(R)h\nu)^2$ is obtained using eqn. 2. The optical band gap is determined by taking $(F(R)h\nu)^2$ *versus* energy of photon (hν) and a stroke is plotted towards the x axis = 0. The optical band gap for $MgFe_2O_4$ nanoferrites prepared in sol-gel, green sol-gel green combustion and combustion methods found to be 2.3, 2.6, 2.7 and 2.8 eV, respectively. In any case, an optimum bandgap will ease excitation of an electron from the valence band to the conduction band in the green sol-gel prepared $MgFe_2O_4$ nanoferrites thus increasing the photocatalytic activity of material. The variation band gap in prepared samples can be ascribed to internal transitions in a partially filled Mg *p*-orbital. It seems clear that *p*-orbitals play a significant role in the photoexcitation and photocatalytic activity.

EIS analysis: Electrochemical behaviour of synthesized nanoferrites was evaluated by electrochemical impedance spectroscopy (EIS). The EIS data comprises a semi-arc at higher frequencies corresponding to resistance and a slope at middle and low frequencies corresponds to capacitance. The acquired nyquist data signified the highly inclined diffusion line for sol-gel prepared $MgFe_2O_4$ nanoferrite which suggests more prominent capacitive behaviour. The nyquist plot around low frequencies tends to vertical axis. The semi-arc formed at high frequencies is due to the consequence of charge transfer resistance introduced in the boundary amid of the porous electrode surface and electrolyte solution [28]. The green sol-gel synthesized $MgFe_2O_4$ nanoferrite exhibited fewer charge transfer resistance related to nanoferrite by other routes (Fig. 5). The charge transfer resistance for nanoferrites synthesized by green sol-gel, sol-gel, SCS and green SCS methods were 32, 51, 97 and 74 Ω, respectively. It noticeably specifies the significant drop in the charge transfer rate which in turn increases the electron-hole pair recombination time. The result justifies that the enhanced efficient photocatalytic activity of green sol-gel $MgFe_2O_4$ nanoferrite.

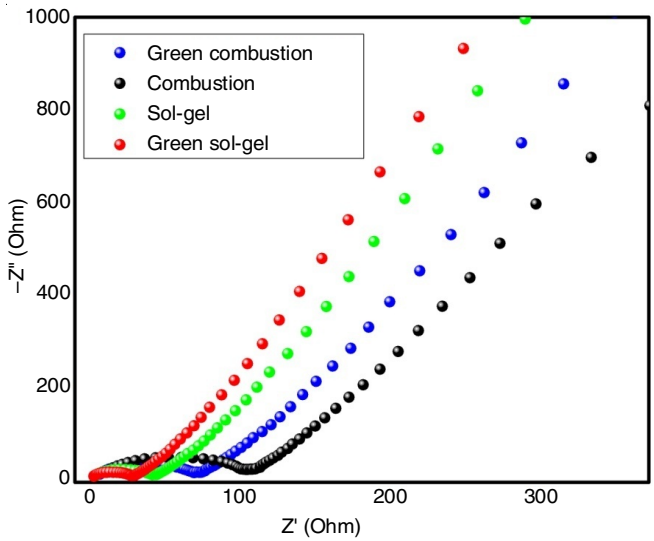

Fig. 5. Impedance plot for nanoferrites synthesized by sol-gel, green sol-gel, SCS and green SCS methods

Photocatalytic analysis: The photocatalytic activity of the prepared materials was examined by degrading the Rose Bengal dye under UV-light irradiation. Photocatalytic reactor was used to conduct the experiment. The dye of 20 ppm in 250 mL of distilled water and 40 g of photocatalyst was added. The reaction mixture was stirred under the illumination of UV-light for 45 min. By analyzing absorption spectra (Fig. 6a-d), $MgFe_2O_4$ nanoferrites prepared by green sol-gel executed a much higher degradation potential than those of other method. log C/C_o *versus* time plot has been displayed for degradation of Rose Bengal dye (Fig. 7a). In the absence of photocatalysts under UV light, there is no significant variation in the concentration of Rose Bengal dye, signifying the inefficiency of self-degradation of Rose Bengal dye molecules. In absence of light source there is no degradation observed. $MgFe_2O_4$ nanoferrites prepared by sol-gel revealed the higher photocatalytic performance with the Rose Bengal dye degradation ratio of 98.6 % in 45 min. On contrary, $MgFe_2O_4$ nanoferrites of green combustion, combustion and sol-gel degraded was 71.5, 66.2 and 80.3 % of Rose Bengal dye, respectively. Hence, it is assumed that the improved photocatalytic activity for composites for green sol-gel nanoferrite is due to the size, optimum band width and less charge transfer resistance.

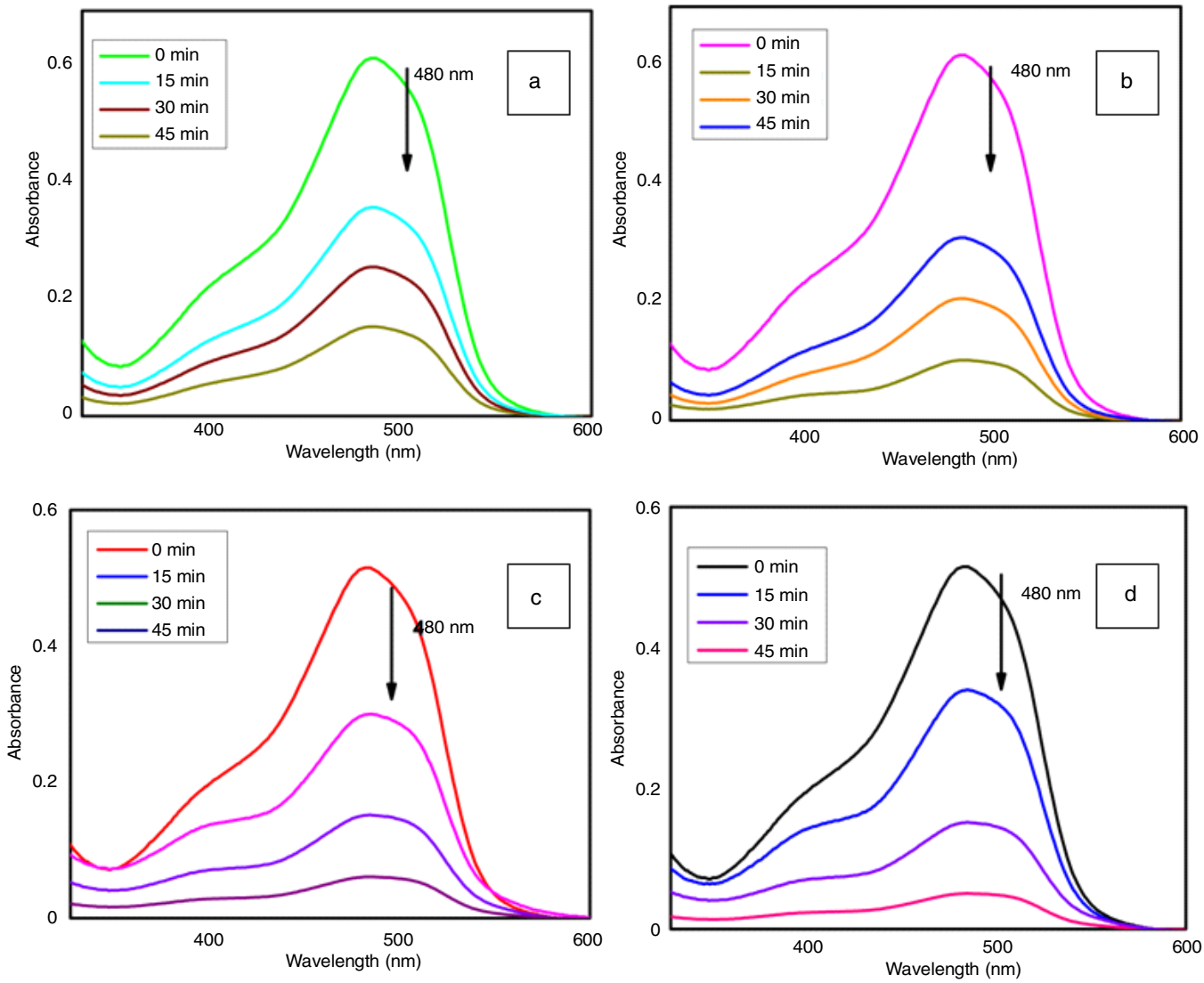

Fig. 6. Absorption spectra for $MgFe_2O_4$ Nanoferrites prepared by (a) combustion, (b) green combustion, (c) sol-gel and (d) green sol-gel methods

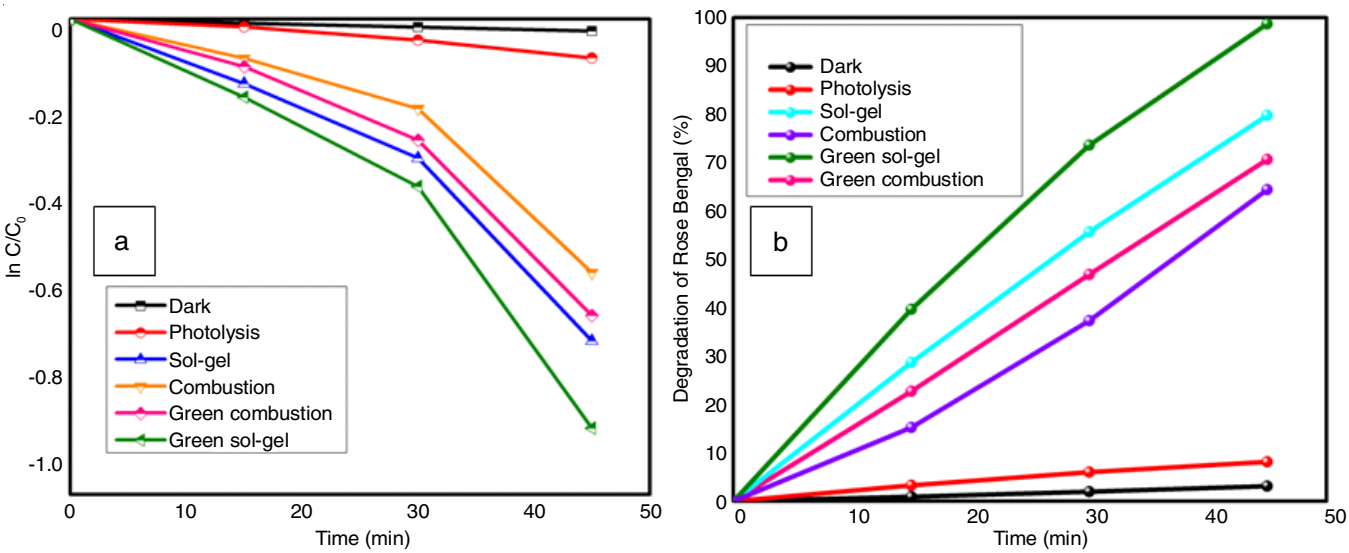

Fig. 7. (a) log C/C_0 *versus* time and (b) percentage degradation of rose bengal for $MgFe_2O_4$ nanoferrites prepared by sol-gel, green sol-gel and combustion, green combustion methods

The maximum removal efficiency in lab scale experiment for an initial concentration of C_o and final concentration C of dye solution after reaction was calculated by following formula:

$$\text{Efficiency } (\%) = \frac{C_o - C}{C_o} \times 100 \quad (3)$$

Photocatalytic mechanism: The valence electrons in $MgFe_2O_4$ nanoferrites get excited to conduction band upon irradiation of UV light (Fig. 8a). After the generation of electron-hole pair, the excited electron reacts with surface oxygen molecule to produce free oxygen radicals. The oxygen radicals react with water molecules to form HO_2^*, later it produces H_2O_2. Likewise, hole reacts with hydroxyl ion of water molecule to generate hydroxyl radicals. These superoxide radicals produced from electron-hole pair reacts with dye molecules. The dye molecules are degraded into CO_2, water and organic ions.

$$MgFe_2O_4 + h\nu \longrightarrow MgFe_2O_4\,(e^- + h^+) \quad (4)$$

$$h^+ + OH \longrightarrow OH^* \quad (5)$$

$$O_2 + e^- \longrightarrow O_2^* \quad (6)$$

$$H_2O + O_2^* \longrightarrow HO_2^* + OH \quad (7)$$

$$H_2O + HO_2^* \longrightarrow H_2O_2 + OH^* \quad (8)$$

$$H_2O_2 \longrightarrow 2OH^* \quad (9)$$

$$O_2^* + OH^* + \text{Rose bengal dye}^* \longrightarrow CO_2 + \text{Water molecule} + \text{Inorganic ions} \quad (10)$$

Recycling experiments were carried out to examine the stability of the photocatalyst so that it can be used for practical applications. To reuse the photocatalyst from the reaction mixture an external bulk magnet is used. The extracted photocatalyst was washed with ethanol and dried for each run. Further, the photocatalyst is used for the next 4 more runs for the degradation of Rose Bengal dye. At the end of experiment, the photocatalyst was extracted again for the further run. The graph is

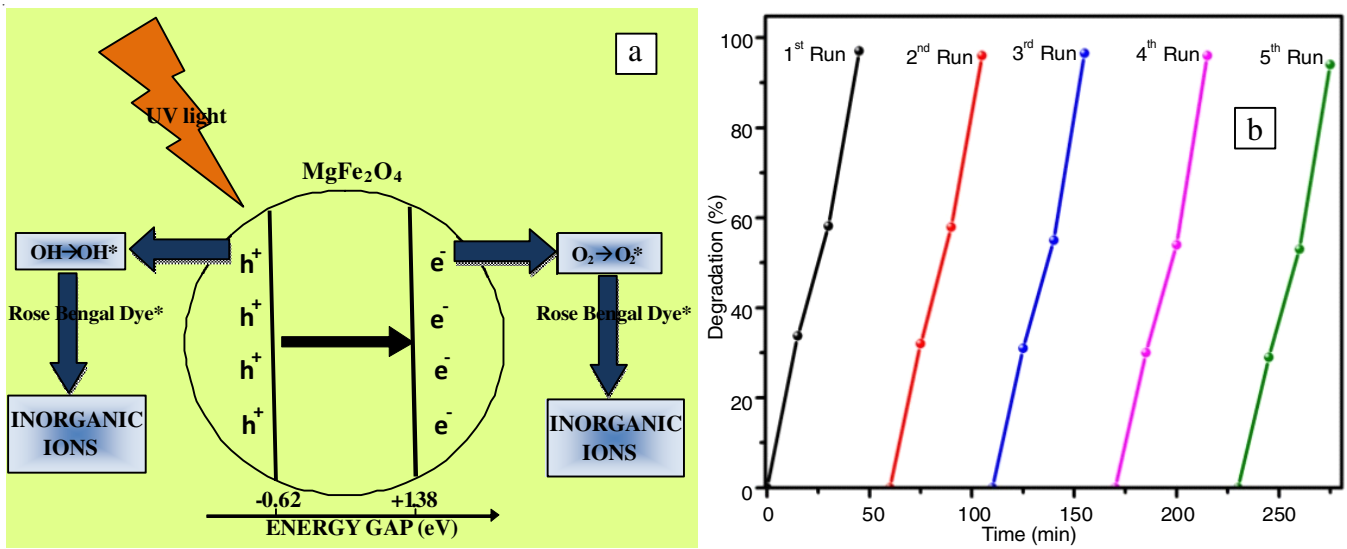

Fig. 8. (a) Mechanism for photocatalytic degradation of dye by $MgFe_2O_4$ NPs, (b) Percentage degradation of Rose Bengal dye by green sol-gel nanoferrites for recycling experiment

plotted for all 5 runs with respect of percentage degradation. (Fig. 8b). The results showed almost consistency in the decomposition rate for all the 5 runs ensuring the stability of photocatalyst.

Conclusion

The synthesized $MgFe_2O_4$ nanoferrites *via* chemical and green methods successfully degraded the Rose Bengal dye under UV light. FTIR and PXRD results gave the specific information regarding the structural composition and crystalline size, respectively for the nanoferrites. DRS signified that $MgFe_2O_4$ nanoferrites can absorb both UV light and visible light, maximum visible light absorption being at 499 nm. Photocatalytic activity of $MgFe_2O_4$ nanoferrites developed by various techniques were compared for the efficient degradation of Rose Bengal dye and $MgFe_2O_4$ nanoferrites prepared by green sol-gel method was confirmed to be competent photocatalyst under UV illumination as compared to other photocatalysts. The EIS spectrum indicates that the higher photocatalytic performance of green sol-gel nanoferrites are usual due to less charge transfer resistance. Major degradation of Rose Bengal dye resulted due to holes as analyzed by scavenging experiment. $MgFe_2O_4$ nanoferrites can be recycled and used at least five times without much change in degradation efficiency. Thus, $MgFe_2O_4$ nanoferrites prepared by green sol-gel method can be exploited for wastewater treatment of dye/textile under UV irradiation.

CONFLICT OF INTEREST

The authors declare that there is no conflict of interests regarding the publication of this article.

REFERENCES

1. D. Cruickshank, *J. Eur. Ceram. Soc.*, **23**, 2721 (2003); https://doi.org/10.1016/S0955-2219(03)00145-6
2. M. Damnjanovic, G. Stojanovic, V. Desnica, L. Zivanov, R. Raghavendra, P. Bellew and N. Mcloughlin, *IEEE Trans. Magn.*, **42**, 270 (2006); https://doi.org/10.1109/TMAG.2005.860485
3. D.G. Mitchell, *J. Magn. Reson. Imaging*, **7**, 1 (1997); https://doi.org/10.1002/jmri.1880070102
4. M.A. Ahmed and S.T. Bishay, *J. Magn. Magn. Mater.*, **279**, 178 (2004); https://doi.org/10.1016/j.jmmm.2004.01.096
5. S.V. Bangale, D.R. Patil and S.R. Bamane, *Arch. Appl. Sci. Res.*, **3**, 506 (2011).
6. W.L. Suchanek and R.E. Riman, *Adv. Sci.Technol.*, **45**, 184 (2006); https://doi.org/10.4028/www.scientific.net/AST.45.184
7. M. Kaur, S. Rana and P.S. Tarsikka, *Ceram. Int.*, **38**, 4319 (2012); https://doi.org/10.1016/j.ceramint.2012.02.013
8. M. Kaur, B.S. Randhawa and P.S. Tarsikka, *Ind. J. Eng. Mater. Sci.*, **20**, 325 (2013).
9. N.D. Kandpal, N. Sah, R. Loshali, R. Joshi and J. Prasad, *J. Sci. Ind. Res. (India)*, **73**, 87 (2014).
10. P. Binu Jacob, A. Kumar, R.P. Pant, S. Singh and E.M. Mohammed, *Bull. Mater. Sci.*, **34**, 1345 (2011).
11. S.T. Fardood, Z. Golfar and A. Ramazani, *J. Mater. Sci. Mater. Electron.*, **28**, 17002 (2017); https://doi.org/10.1007/s10854-017-7622-y
12. S. Kumar, A. Sharma, M. Singh and S.P. Sharma, *Arch. Phys. Res.*, **5**, 18 (2014).
13. S. Kaviya, J. Santhanalakshmi, B. Viswanathan, J. Muthumary and K. Srinivasan, *Spectrochim. Acta A: Mol. Biomol. Spectrosc.*, **79**, 594 (2011); https://doi.org/10.1016/j.saa.2011.03.040
14. O.B. Garcia, J. Castillo, J.R. Marin, A. Ortuno and J.A. Del Rio, *J. Agric. Food Chem.*, **45**, 4505 (1997); https://doi.org/10.1021/jf970373s
15. J.A. Vinson, X. Su, L. Zubik and P. Bose, *J. Agric. Food Chem.*, **49**, 5315 (2001); https://doi.org/10.1021/jf0009293
16. D. Gingasu, I. Mîndru, S. Preda, J.M. Calderon-Moreno, D.C. Culita, L. Patron and L. Diamandescu, *Rev. Roum. Chim.*, **62**, 645 (2017).
17. S.S. Devi and S.B. Paul, *Biol. Environ. Sci.*, **7**, 156 (2011).
18. E. Casbeer, V.K. Sharma and X.Z. Li, *Sep. Purif. Technol.*, **87**, 1 (2012); https://doi.org/10.1016/j.seppur.2011.11.034
19. H.G. Kim, P.H. Borse, J.S. Jang, E.D. Jeong, O.S. Jung, Y.J. Suh and J.S. Lee, *Chem. Commun.*, **39**, 5889 (2009); https://doi.org/10.1039/b911805e
20. L. Zhang, Y. He, Y. Wu and T. Wu, *Sci. Eng. B*, **176**, 1497 (2011); https://doi.org/10.1016/j.mseb.2011.09.022
21. S. Maensiri, M. Sangmanee and A. Wiengmoon, *Nanoscale Res. Lett.*, **4**, 221 (2009); https://doi.org/10.1007/s11671-008-9229-y
22. Y.-S. Fu, X.-W. Du, S.A. Kulinich, J.-S. Qiu, W.-J. Qin, R. Li, J. Sun and J. Liu, *J. Am. Chem. Soc.*, **129**, 16029 (2007); https://doi.org/10.1021/ja075604i
23. Y.S. Vidya, K.S. Anantharaju, H. Nagabhushana and S.C. Sharma, *J. Alloys Compd.*, **619**, 760 (2015); https://doi.org/10.1016/j.jallcom.2014.09.050
24. V.A.M. Brabers, *Phys. Status Solidi*, **33**, 563 (1969); https://doi.org/10.1002/pssb.19690330209
25. K. Shetty, S.V. Lokesh, D. Rangappa, H.P. Nagaswarupa, H. Nagabhushana, K.S. Anantharaju, S.C. Prashantha, Y.S. Vidya and S.C. Sharma, *Physica B*, **507**, 67 (2017); https://doi.org/10.1016/j.physb.2016.11.021
26. D.M. Jnaneshwara, D.N. Avadhani, B.D. Prasad, H. Nagabhushana, B.M. Nagabhushana, S.C. Sharma, S.C. Prashantha and C. Shivakumara, *Spectrochim. Acta Mol. Biomol. Spectrosc.*, **132**, 256 (2014); https://doi.org/10.1016/j.saa.2014.04.179
27. D.M. Jnaneshwara, D.N. Avadhani, B.D. Prasad, B.M. Nagabhushana, H. Nagabhushana, S.C. Sharma, S.C. Prashantha and C. Shivakumara, *J. Alloys Compd.*, **587**, 50 (2014); https://doi.org/10.1016/j.jallcom.2013.10.146
28. J. Roncali, *Chem. Rev.*, **92**, 711 (1992); https://doi.org/10.1021/cr00012a009